ISSN 0021-3640, JETP Letters, 2006, Vol. 83, No. 11, pp. 488–492. © Pleiades Publishing, Inc., 2006.
Original Russian Text © Y.K. Fetisov, C.E. Patton, V.T. Synogach, 2006, published in Pis'ma v Zhurnal Éksperimental'noĭ i Teoreticheskoĭ Fiziki, 2006, Vol. 83, No. 11, pp. 579–583.

Envelope Solitons in a Medium with Strong Nonlinear Damping

Y. K. Fetisov[a], C. E. Patton[b], and V. T. Synogach[b]

[a] *Moscow State Institute of Radioengineering, Electronics, and Automation (Technical University), pr. Vernadskogo 78, Moscow, 119454 Russia*
e-mail: fetisov@mirea.ru

[b] *Department of Physics, Colorado State University, Fort Collins, Colorado 80523, USA*

Received February 9, 2006; in final form, April 26, 2006

The formation of microwave spin-wave envelope solitons in the ferrite film of yttrium iron garnet in the presence of strong nonlinear damping has been experimentally found and investigated. The solitons are formed due to the four-wave interactions of spin waves when the characteristic time of wave modulation-instability development is much shorter than the time for establishing the generation of short-wavelength magnons. The presence of nonlinear damping allows the excitation of spin-wave envelope solitons by means of long microwave pulses.

PACS numbers: 75.30.Ds

DOI: 10.1134/S002136400611004X

Envelope solitons are wave packets that propagate in a nonlinear dispersive medium, conserving its shape. Envelope solitons are formed from short exciting pulses with sufficiently large amplitude due to competition between dispersive spreading and nonlinear compression. In an ideal dissipationless medium, the stationary form of the soliton is achieved at infinite distance from the excitation point.

The formation and propagation of envelope solitons were experimentally observed in nonlinear dispersive media with low damping: optical solitons in nonlinear optical fibers [1] and microwave spin-wave solitons in ferrite films [2, 3]. It was shown that weak damping leads to a qualitative change in the properties of solitons compared to the ideal dissipationless medium. In particular, a soliton is formed at a finite distance from the excitation point and the power of the propagating soliton decreases twice as fast as the power of a small-amplitude linear pulse [4].

In this work, it has been shown experimentally that envelope solitons can also be formed and propagate in media with strong nonlinear damping. The existence of solitons in such media is possible if the characteristic time of modulation-instability development, which gives rise to the formation of solitons, is shorter than the time of establishing nonlinear damping. In this case, the threshold power for the appearance of modulation instability can be much higher than the threshold power for the appearance of nonlinear damping. Owing to the effect of nonlinear damping, the envelope soliton can be formed from a long exciting pulse.

The effect is illustrated on the example of bulk spin waves propagating in tangentially magnetized ferrite films along the magnetic field direction. For these waves, the conservation laws allow two kinds of four-wave interactions, which are responsible for both modulation instability and nonlinear damping of spin waves.

A standard transmission line based on spin waves was used [5]. The line consisted of a 25×2-mm rectangular yttrium iron garnet (YIG) film 5.1 μm in thickness and two microstrip transducers for the excitation and receipt of spin waves. The film was grown by liquid-phase epitaxy on a nonmagnetic substrate 0.5 mm in thickness and had a saturation magnetization of 1750 G and the linewidth 0.4 Oe of uniform ferromagnetic resonance at a frequency of 5 GHz. Transducers 2 mm in length and 50 μm in width were produced by the photolithography method on polycore substrates. Each transducer was connected with a 50-Ω line at one end and was shorted at the other end. The distance l between the transducers, which determined the wave propagation length, could be varied from 1.5 to 10 mm by displacing one of the substrates. The YIG film was applied on the transducers and the entire structure was placed in a constant external magnetic field directed along the long axis of the film and perpendicularly to the transducers. A continuous or pulsed microwave signal with a frequency in a range of 3.5–10 GHz and a power up to 500 mW was fed to the input transducer of the transmission line and the characteristics of the signal from the output transducer were measured for a field range of 0.6–3 kOe.

Figure 1 shows the frequency response curve, i.e., the dependence of insertion loss in the transmission line $L = 10\log(P_{out}/P_{in})$ (P_{in} and P_{out} are the input and output powers, respectively) on the signal frequency f, which is measured in the continuous exciting-signal regime

for a field of H = 1000 Oe and the distance between transducers l = 3.4 mm. Lines *1* and *2* correspond to low- and high-power input signals P_{in} = 10 μW and 200 mW. For low power P_{in}, spin waves are excited and propagate in a frequency range of 4.45–4.83 GHz and the minimum insertion loss is equal to –24 dB. The shape and boundaries of the frequency response curve of the transmission line for low power are well reproduced by the theory developed in [3] if H = 1060 Oe. The difference of measured and calculated H values is explained by the effect of the anisotropy of the YIG film.

As the power P_{in} of the input signal increases, the insertion loss L increases sharply at all frequencies within the frequency response curve of the transmission line (see Fig. 1, line *2*). This behavior indicates that strong nonresonant nonlinear damping of waves appears. An increase in the damping of waves with P_{in} is observed for all frequencies from 3.5 to 10 GHz when the field varies from 0.6 to 3 kOe.

Figure 2 shows the typical dependence of the signal power P_{out} at the output of the transmission line on the power P_{in} of the continuous input signal of a frequency of f_0 = 4.77 GHz in a field of H = 1000 Oe. It is seen that P_{out} increases linearly with the input power up to the threshold value $P_{in}^{dam} \approx 4$ mW. As P_{in} increases further, the output power is saturated and remains constant equal to $P_{out}^{sat} \approx 20$ μW. This dependence indicates that the strong nonlinear damping of waves appears for $P_{in} > P_{in}^{dam}$. Similar curves are obtained for all frequencies in the spin-wave excitation range. The threshold power P_{in}^{dam} at which nonlinear damping appears varies slightly when the magnetic field and wave frequency are rearranged.

The propagation of spin wave pulses in the transmission line is investigated for H = 1000 Oe and the distance between transducers l = 3.4 mm. Rectangular exciting pulses have a central frequency of f_0 = 4.77 GHz, a duration of 0.7 μs, and increasing and decreasing times shorter than 2 ns. The pulses follow with an interval of 10 ms, which makes it possible to avoid the absorbing-power-induced heating of the film. Figure 3 shows the typical shape of the output-pulse envelope for various powers P_{in} of the input pulses. For a low power P_{in}, the shape of the output pulse repeats the shape of the exciting pulses with a delay of 0.15 μs (see Fig. 3a). As P_{in} increases, an interval of the exponential power decrease appears at the peak of the output pulse (see Fig. 3b). The output power decreases from P_{out}^{max} at the beginning of the pulse to P_{out}^{sat} on the flat peak at the end of the pulse. As P_{in} increases, the interval of the exponential output-power decrease becomes shorter. The characteristic time of the exponential output-power decrease reaches a minimum of ~50 ns for

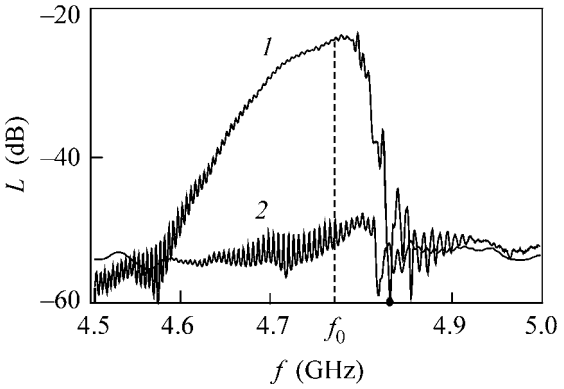

Fig. 1. Insertion loss L in the transmission line vs. the exciting signal frequency f in the continuous regime for low and high powers P_{in} = (*1*) 10 μWand (*2*) 200 mW in a magnetic field of H = 1000 Oe for the distance between transducers l = 3.4 mm and f_0 = 4.77 GHz.

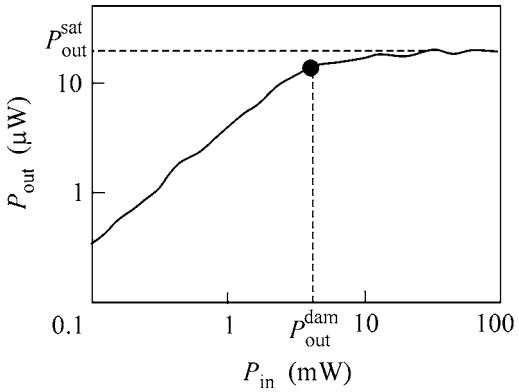

Fig. 2. Signal power P_{out} at the output of the transmission line vs. the power P_{in} of the continuous input signal for f_0 = 4.77 GHz, H = 1000 Oe, and l = 3.4 mm. The threshold power for the appearance of nonlinear damping P_{in}^{dam} = 4 mW and the output-signal saturation power $P_{out}^{sat} \approx 20$ μW.

$P_{in} \approx 30$ mW. The interval of the exponential output-power decrease is followed by the interval of the constant power $P_{out}^{sat} \approx 20$ μW, which is equal to the power saturation level in the continuous signal regime (see Fig. 2). For input powers $P_{in} \geq 30$ mW, a narrow peak with an FWHM of about 15 ns is formed at the beginning of the output pulse (see Figs. 3d and 3e). The remaining part of the exponential interval, which is observed for low input powers, is seen in Fig. 3e.

The narrow peak at the beginning of the output pulse in Fig. 3d is a spin-wave envelope soliton, which is formed from a long exciting pulse. Additional measurements were carried out in order to confirm the soliton nature of this peak.

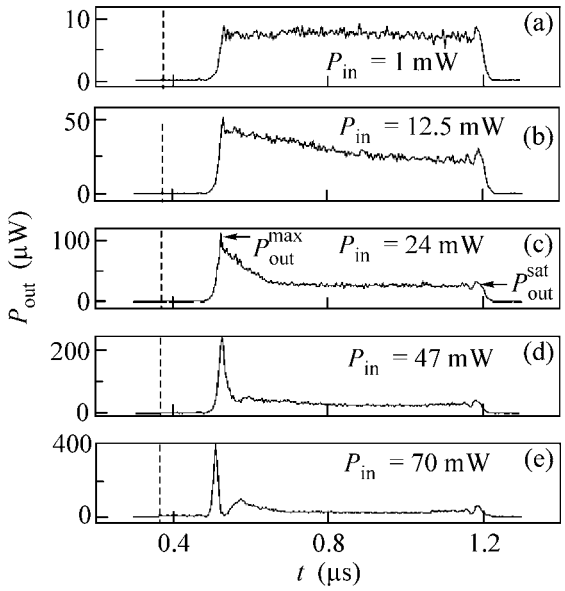

Fig. 3. Evolution of the spin-wave pulse envelope with increasing the exciting-pulse power P_{in}. The exciting-pulse duration is equal to 0.7 μs. The vertical dashed straight lines indicate the beginning of the exciting pulse; P_{out}^{max} and P_{out}^{sat} are the powers of the peak at the beginning of the pulse and in its flat interval, respectively.

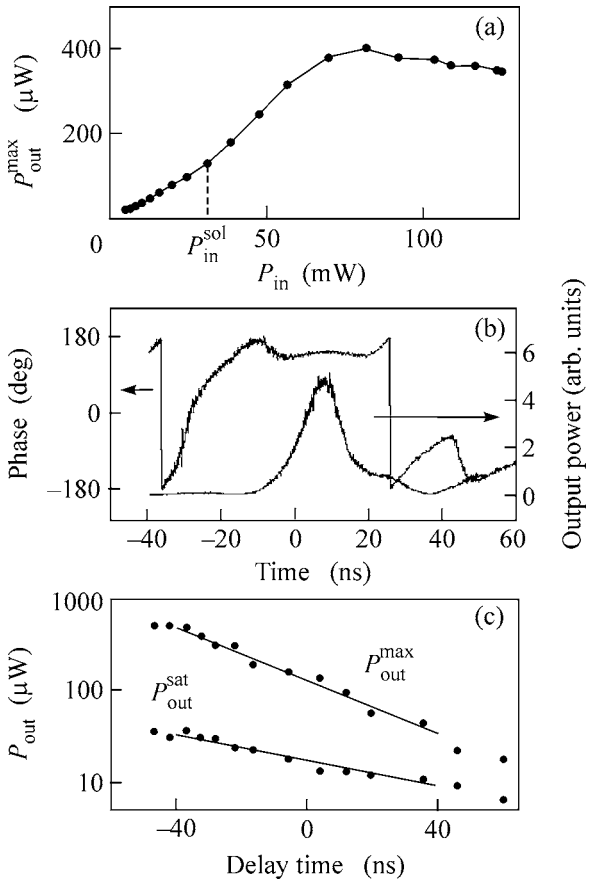

Fig. 4. Characteristics of the spin-wave envelope soliton, which is excited by a pulse with a duration of 0.7 μs and a power of P_{in} = 56 mW. (a) Maximum soliton power P_{out}^{max} vs. the exciting-pulse power P_{in}, (b) the envelope shape and phase characteristic of the soliton, and (c) the soliton power P_{out}^{max} and output-pulse saturation power P_{out}^{sat} vs. the wave propagation time. The points are the experimental data and the solid lines are the exponential approximations of the data.

Figure 4a shows the maximum power P_{out}^{max} measured as a function of the input power under the same conditions as the data shown in Fig. 3. The line exhibits a characteristic kink at $P_{in} \approx 30$ mW, which corresponds to the beginning of the nonlinear compression of the output pulse. For powers $P_{in} \sim 70$ mW and higher, the peak height ceases to increase and even decreases slightly. The line completely repeats a similar dependence for a spin-wave envelope soliton that is formed from a short exciting pulse [6]. According to Fig. 4a, the threshold power for the soliton formation is equal to $P_{in}^{sol} \approx 30$ mW.

Figure 4b shows the time dependence of the phase distribution in the region of the output-pulse peak that is measured at $P_{in} = 56$ mW and under the same conditions as the data given in Fig. 3. It is seen that the phase remains constant within the peak interval. This property also confirms the soliton nature of the observed pulse [7].

Figure 4c shows the maximum peak power P_{out}^{max} and the power P_{out}^{sat} on the flat peak at the end of the output pulse as functions of the wave propagation time in the transmission line for an exciting pulse power of $P_{in} = 56$ mW. The propagation time increases from 83 to 350 ns when the distance between the transducers of the line is increased from 1.9 to 8 mm, which corresponds to the calculated group velocity of the waves $V_g = 2.3 \times 10^6$ cm/s. The solid lines are the exponential approximations of the data for propagation times of 100–300 ns. Both dependences are linear on a semilogarithmic scale. The decrease rate of the maximum power P_{out}^{max} is equal to 57.8 dB/μs, which is higher than the decrease rate of the flat-peak pulse power P_{out}^{sat} = 28 dB/μs by a factor of 2.07. The flat peak of the output pulse can be treated as a small-amplitude continuous wave. The result obtained above is consistent with the theoretical prediction and the experimental data indicating that the damping rate of a spin-wave envelope soliton is twice as high as the value for the linear wave in YIG films [8].

In order to explain the mechanism of the formation of the envelope soliton from a long exciting pulse, we analyze the dispersion characteristic of bulk spin waves

in a tangentially magnetized film. The frequency f of the fundamental mode of bulk waves calculated by the formulas taken from [3] with $H = 1060$ Oe and parameter values satisfying the experimental conditions is shown in Fig. 5 as a function of the wavenumber k whose axis is given on a logarithmic scale. The dispersion curve consists of the part for low wavenumbers $k < 10^4$ rad/cm, where the dipole interaction prevails, and the part for high wavenumbers $k > 10^5$ rad/cm, where the exchange interaction prevails. The central frequency and central wavenumber of the input wave packet are indicated as f_0 and k_0, respectively. Half the frequency of the exciting signal is denoted as $f_0/2$.

According to Fig. 5, the conservation laws allow only the four-wave interactions of waves with frequencies close to f_0. The three-wave interactions for which the wave with the initial frequency f_0 splits into two waves with frequencies close to $f_0/2$ are forbidden, because the halved frequency is much lower than the frequencies of exciting spin waves. In this case, two kinds of four-wave interactions are possible.

First, the spin wave with the frequency f_0 and wave vector $\mathbf{k}_0$ can excite short-wavelength magnons if its power exceeds a certain threshold. The frequency of the magnons is close to f_0 and their wavenumbers belong to the exchange part of the dispersion curve as shown in Fig. 5. The energy and momentum conservation laws for these processes have the form $2f_0 = f_1 + f_2$ and $2\mathbf{k}_0 = \mathbf{k}_1 + \mathbf{k}_2$, respectively, where f_1 and f_2 are the frequencies of the magnons and $\mathbf{k}_1$ and $\mathbf{k}_2$ are their wave vectors. The energy transfer from the spin wave to the short-wavelength magnons is responsible for the damping of the wave. As seen in Fig. 2, the threshold power for the appearance of nonlinear damping was equal to $P_{\text{in}}^{\text{dam}} = 4$ mW in our experiments. This value is in agreement with the saturation power measured and calculated for bulk spin waves in ferrite films [9].

Second, the Lighthill criterion ($DN < 0$, where D and N are the dispersion and nonlinear coefficients, respectively) is valid for bulk spin waves and modulation-instability development is possible for them [10]. Modulation instability appears if the wave power exceeds the second threshold level. The conservation laws for this process have the similar form $2f_0 = f_3 + f_4$ and $2\mathbf{k}_0 = \mathbf{k}_3 + \mathbf{k}_4$, where f_3 and f_4 are the frequencies of the generated waves and $\mathbf{k}_3$ and $\mathbf{k}_4$ are their wave vectors. The wavenumbers of waves generated in the presence of modulation instability are approximately equal to the wavenumber of the initial wave (k_3, $k_4 \approx k_0$) and belong to the dipole part of the dispersion curve as shown in Fig. 5. Modulation instability is responsible for the formation of a spin-wave envelope soliton. The threshold power for the formation of the soliton in our experiments is equal to $P_{\text{in}}^{\text{sol}} \approx 30$ mW. The measured $P_{\text{in}}^{\text{sol}}$ value should be compared to the calculated power

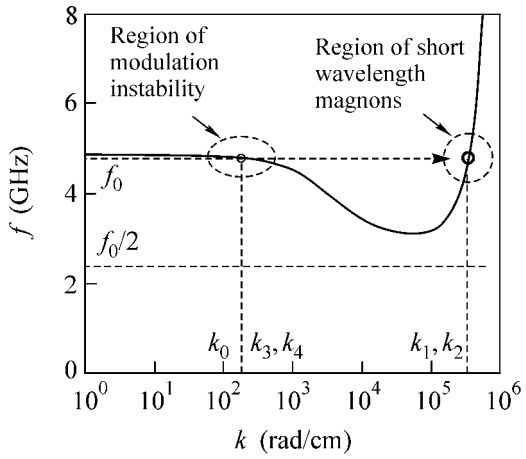

Fig. 5. Dispersion curve for the fundamental mode of bulk spin waves in a tangentially magnetized YIG film 5.1 μm. The horizontal dashed straight lines show the wave frequency f_0 and halved frequency $f_0/2$, k_0 is the initial wavenumber, k_1 and k_2 are the wavenumbers of short-wavelength magnons, and k_3 and k_4 are the wavenumbers of modulationally instable waves. The nonlinear damping and modulation-instability regions are indicated by circles.

required for the formation of the soliton from a short exciting pulse. The calculation by the formulas taken from [9] with the inclusion of a loss of –10 dB in the microstrip transducer, an exciting-pulse duration of 15 ns, and the values of other parameters corresponding to the experimental conditions yields a value of 22 mW for the threshold power for the soliton formation, in agreement with experiment.

The described four-wave processes of the nonlinear damping and modulation instability of spin waves are jointly responsible for the formation of envelope solitons from a long exciting pulse. If the input power exceeds the threshold value $P_{\text{in}}^{\text{dam}}$, nonlinear damping leads only to the shortening of the wave packet to several tens of nanosecond, as shown in Fig. 3c. If the input power exceeds the threshold value $P_{\text{in}}^{\text{sol}}$, nonlinear damping leads to the shortening of the wave packet and modulation instability "cuts" the exponential interval and, using this quite short pulse, forms the envelope soliton with a duration of about 15 ns, as shown in Fig. 3e.

In the described experiments, the threshold power for the appearance of modulation instability that leads to the formation of solitons is higher than the threshold power for nonlinear damping processes by a factor of $P_{\text{in}}^{\text{sol}}/P_{\text{in}}^{\text{dam}} = 7.5$. However, the characteristic time of modulation-instability development (~8 ns) appears to be much shorter than the characteristic time of the development of nonlinear damping processes (~50 ns). This ratio of the times ensures the possibility of forming envelope solitons in the presence of strong nonlinear damping. We emphasize that the shortening of

pulses due to nonlinear damping complicates the observation of multisoliton regimes of the propagation of bulk spin-wave pulses in tangentially magnetized YIG films.

We are grateful to A.I. Maĭmistov for stimulating discussions. This work was supported by INTAS, the Ministry of Education and Science of the Russian Federation, and the U.S. National Science Foundation.

REFERENCES

1. G. P. Agrawal, *Nonlinear Fiber Optics*, 2nd ed. (Academic, San Diego, 1995; Mir, Moscow, 1996), Chap. 5.
2. B. A. Kalinikos, N. G. Kovshikov, and A. N. Slavin, Pis'ma Zh. Éksp. Teor. Fiz. **38**, 343 (1983) [JETP Lett. **38**, 413 (1983)].
3. A. N. Slavin, B. A. Kalinikos, and N. G. Kovshikov, in *Nonlinear Phenomena and Chaos in Magnetic Materials*, Ed. by P. E. Wigen (World Sci., Singapore, 1994), Chap. 9.
4. A. Nasegawa and Y. Kodama, Proc. IEEE **69**, 1145 (1981).
5. M. Chen, M. A. Tsankov, J. M. Nash, and C. E. Patton, Phys. Rev. B **49**, 12 773 (1994).
6. P. De Gasperis, R. Marcelli, and G. Miccolli, Phys. Rev. Lett. **59**, 481 (1987).
7. J. M. Nash, P. Kabos, R. Staudinger, and C. E. Patton, J. Appl. Phys. **83**, 2689 (1988).
8. B. A. Kalinikos, N. G. Kovshikov, and A. N. Slavin, IEEE Trans. Magn. **28**, 3207 (1992).
9. N. Guan, T. Maruyama, K. Yashiro, et al., in *Proceedings of the 6th International Conference on Ferrites* (Tokyo, 1992), p. 1362.
10. A. K. Zvezdin and A. F. Popkov, Zh. Éksp. Teor. Fiz. **84**, 606 (1983) [Sov. Phys. JETP **57**, 350 (1983)].

Translated by R. Tyapaev